J. Membrane Biol. 27, 131–151 (1976)

New Membrane Formation and Intercellular Communication in the Early *Xenopus* Embryo

II. Theoretical Analysis

S. W. de Laat and P. W. J. A. Barts

Hubrecht Laboratory, International Embryological Institute, Utrecht, The Netherlands

Received 2 January 1975; revised 9 September 1975

Summary. In conjunction with a previous analysis of the electrical networks formed by the *Xenopus* embryo during development from the 2-cell stage to the 16-cell stage, some theoretical aspects are investigated. A computer simulation method for the derivation of the specific membrane resistances from the measured equivalent resistances between different compartments of a multicellular biological system is described in detail. The interdependence of the equivalent junctional and nonjunctional resistances, and the possible role of the blastocoel in intercellular communication are analyzed. Assuming that no direct pathways exist between nonadjacent cells, the equivalent junctional and nonjunctional resistances, as well as the resulting coupling ratios are calculated for all pairs of cells in the 4-cell, 8-cell and 16-cell embryo. Previous studies on electrotonic coupling in the early *Xenopus* embryo are discussed.

In a preceding article [4] we presented the results of an electrophysiological investigation of intercellular communication during the development of *Xenopus laevis* embryos from the 2-cell stage to the 16-cell stage. The equivalent junctional resistances and equivalent nonjunctional resistances were measured continuously in pairs of adjacent animal cells separated by the different cleavage membranes. The equivalent resistances are a measure for the ion-exchange possibilities between two compartments independent of the pathways involved. They depend on the geometry of the system and on the permeability properties of the individual membranes. The specific resistances of the successively formed cleavage membranes and of the nonjunctional membranes as a function of developmental stage were derived from these data. A computer simulation method was developed for this purpose. This method has general applicability for those systems in which the geometry does not permit the derivation of simple equations describing the spreading of current in the system.

The specific resistances are a measure for the ionic permeability per unit membrane area. The specific resistances of all cleavage membranes

remained constant at about 400 $\Omega\,cm^2$ after an initial increase during the period of membrane formation. It has been argued [4] that the electrophysiological data can be explained without assuming the presence of specialized low-resistance junctions in the intercellular membranes. However, the existence of such junctions, at the stages investigated, could not be excluded.

The equivalent junctional resistances increased stepwise during each cleavage cycle as a result of the formation of new intercellular membranes and the consequent decrease in surface area of the junctional membranes. At the onset of each cleavage cycle no significant differences were found beween the equivalent junctional resistances as measured in different pairs of adjacent cells.

The specific resistance of all nonjunctional membranes decreased from 43.5 $k\Omega cm^2$ in the uncleaved egg [5] to about 10 $k\Omega cm^2$ at the 16-cell stage, due to the insertion of small fractions of the relatively permeable newly formed membranes into the outer surface. It moreover showed a transient decrease during each cleavage cycle due to a temporary separation of the peripheral parts of the blastomeres. The equivalent nonjunctional resistance showed the same pattern of change, and no significant differences were found between different animal cells.

In the present study we give the details of the simulation method used for the derivation of the specific membrane resistances. The interdependence of the equivalent junctional and nonjunctional resistances is analyzed for the *Xenopus* embryo. Furthermore, the possible implications of some of the assumptions made in modelling the *Xenopus* embryo are investigated. On the basis of the experimental data presented in the foregoing paper [4], the simulation method is used for a more detailed analysis of the electrical network that may represent the *Xenopus* embryo at the stages investigated.

Materials and Methods

Notations Used in the Text

A multicellular biological system with n compartments can be represented by a linear electrical network with $m=n+1$ nodes. Voltages are measured with respect to the surrounding medium (node 0). A k-cell embryo has $n=k+1$ compartments: k cells (nodes 1 to $n-1$) and the blastocoel (node n). The following notations are used:

A_{pq}: surface area of the membrane between the adjacent nodes p and q, (cm^2)
j_{ii}: current used for excitation of the network at node i, (amps)
j_{pq}: current flowing from node p to the adjacent node q, (amps)

a: distance between the third cleavage plane and the center of the embryo, (cm)
b: distance between the third cleavage plane and the center of the blastocoel, (cm)
r_i: specific resistance of cleavage membrane i; in a 16-cell embryo $i=$I, II, III, IV, respectively, (Ω cm^2)
r_{pq}: specific resistance of the membrane between the adjacent nodes p and q, (Ω cm^2)
r_n: specific resistance of the membranes enclosing the blastocoel, (Ω cm^2)
r_0: specific resistance of the nonjunctional membranes, (Ω cm^2)
R_{jk}: resistance connecting node j and node k, (Ohm)
R_i': equivalent junctional resistance between two adjacent cells, connected by cleavage membrane i; in the 16-cell embryo $i=$I, II, III, IV, respectively. At least one of the two cells is an animal cell, (Ohm)
R_{ij}': equivalent resistance between node i and node j, (Ohm)
R_0': equivalent nonjunctional resistance between an animal cell and the medium, (Ohm)
v_{ij}: voltage in node j with respect to node 0, caused by the excitation current j_{ii}, (V)
x: radius of the embryo, (cm)
y: radius of the blastocoel, (cm)
y_{pq}: admittance connecting node p and node q, (Ohm^{-1})
y_{ij}': equivalent admittance between node i and node j, (Ohm^{-1})

The Equivalent Resistances Between Nodes of a Passive Network

For a passive electrical network with m nodes, where each node p is connected to each node q via an admittance y_{pq}, and voltages in node 1 to n ($n=m-1$) are measured with respect to node 0, we define:

j_{ii}: the amplitude of the current used for excitation of the network at node i
v_{ij}: the amplitude of the voltage at node j caused by j_{ii}
y_{pq}: The admittance between node p and node q when a current j_{pq} flows from p to q. Since rectification is absent: $y_{pq}=y_{qp}$.

Excitation of the network at node 1 will give the following set of Kirchhoff-equations:

$$\begin{aligned} j_{11} &= j_{10}+j_{12}+\cdots+j_{1n} \\ 0 &= j_{20}+j_{21}+\cdots+j_{2n} \\ &\vdots \quad \vdots \quad \vdots \quad\quad \vdots \\ 0 &= j_{n0}+j_{n1}+\cdots+j_{n(n-1)} \end{aligned} \tag{1}$$

or

$$\begin{aligned} j_{11} &= (v_{11}-v_{10})y_{10}+(v_{11}-v_{12})y_{12}+\cdots+(v_{11}-v_{1n})y_{1n} \\ 0 &= (v_{12}-v_{10})y_{20}+(v_{12}-v_{11})y_{21}+\cdots+(v_{12}-v_{1n})y_{2n} \\ &\vdots \quad\quad\quad \vdots \quad\quad\quad\quad \vdots \quad\quad\quad\quad\quad \vdots \\ 0 &= (v_{1n}-v_{10})y_{n0}+(v_{1n}-v_{11})y_{n1}+\cdots+(v_{1n}-v_{1(n-1)})y_{n(n-1)}. \end{aligned} \tag{2}$$

Voltages are measured with respect to node 0, thus $v_{10}=0$. Furthermore we define:

$$y_{ii}=\sum_{\substack{q=0 \\ q\neq i}}^{n} y_{iq}. \tag{3}$$

Eqs. (2) can now be written in matrix notation:

$$\begin{bmatrix} y_{11} & -y_{12} & \cdots & -y_{1n} \\ -y_{21} & y_{22} & \cdots & -y_{2n} \\ \vdots & \vdots & & \vdots \\ -y_{n1} & -y_{n2} & \cdots & y_{nn} \end{bmatrix} \cdot \begin{bmatrix} v_{11} \\ v_{12} \\ \vdots \\ v_{1n} \end{bmatrix} = \begin{bmatrix} j_{11} \\ 0 \\ \vdots \\ 0 \end{bmatrix}. \tag{4}$$

In a similar way the matrix equation for excitation at node 2 can be derived:

$$\begin{bmatrix} y_{11} & -y_{12} & \cdots & -y_{1n} \\ -y_{21} & y_{22} & \cdots & -y_{2n} \\ \vdots & \vdots & & \vdots \\ -y_{n1} & -y_{n2} & \cdots & y_{nn} \end{bmatrix} \cdot \begin{bmatrix} v_{21} \\ v_{22} \\ \vdots \\ v_{2n} \end{bmatrix} = \begin{bmatrix} 0 \\ j_{22} \\ \vdots \\ 0 \end{bmatrix}. \tag{5}$$

By successive excitation of the network with the currents $j_{11}, j_{22}, \ldots j_{nn}$, and combination of the resulting n matrix equations we obtain:

$$\begin{bmatrix} y_{11} & -y_{12} & \cdots & -y_{1n} \\ -y_{21} & y_{22} & \cdots & -y_{2n} \\ \vdots & \vdots & & \vdots \\ -y_{n1} & -y_{n2} & \cdots & y_{nn} \end{bmatrix} \cdot \begin{bmatrix} v_{11} & v_{21} & \cdots & v_{n1} \\ v_{12} & v_{22} & \cdots & v_{n2} \\ \vdots & \vdots & & \vdots \\ v_{1n} & v_{2n} & \cdots & v_{nn} \end{bmatrix} = \begin{bmatrix} j_{11} & 0 & \cdots & 0 \\ 0 & j_{22} & \cdots & 0 \\ \vdots & \vdots & & \vdots \\ 0 & 0 & \cdots & j_{nn} \end{bmatrix} \tag{6}$$

or in short form:

$$[Y] \cdot [V] = [J]. \tag{7}$$

For the calculation of the equivalent admittances between node i and node j of the network (y'_{ij}) and between each of these nodes and node 0 (y'_{i0} and y'_{j0}), the m-node network is reduced to a network with three nodes. The derivation is given for node 1 and node 2.

When the network is successively excited via node 1 and node 2, Eq. (6) can be written as:

$$\begin{bmatrix} [Y_{11}] & [Y_{12}] \\ [Y_{21}] & [Y_{22}] \end{bmatrix} \cdot \begin{bmatrix} [V_{11}] \\ [V_{12}] \end{bmatrix} = \begin{bmatrix} [J_{11}] \\ [0] \end{bmatrix} \tag{8}$$

where $[Y_{ij}]$, $[V_{ij}]$ and $[J_{ij}]$ are submatrices of $[Y]$, $[V]$ and $[J]$, respectively:

$$[Y_{11}] = \begin{bmatrix} y_{11} & -y_{12} \\ -y_{21} & y_{22} \end{bmatrix} \tag{9}$$

$$[Y_{12}] = \begin{bmatrix} -y_{13} & \cdots & -y_{1n} \\ -y_{23} & \cdots & -y_{2n} \end{bmatrix}. \tag{10}$$

$[Y_{21}]$ is the transposed matrix of $[Y_{12}]$:

$$[Y_{21}] = [\bar{Y}_{12}] \tag{11}$$

$$[Y_{22}] = \begin{bmatrix} y_{33} & \cdots & -y_{3n} \\ \vdots & & \vdots \\ -y_{n3} & \cdots & y_{nn} \end{bmatrix} \tag{12}$$

$$[V_{11}] = \begin{bmatrix} v_{11} & v_{21} \\ v_{12} & v_{22} \end{bmatrix} \tag{13}$$

$$[V_{12}] = \begin{bmatrix} v_{13} & v_{23} \\ \vdots & \vdots \\ v_{1n} & v_{2n} \end{bmatrix} \tag{14}$$

$$[J_{11}] = \begin{bmatrix} j_{11} & 0 \\ 0 & j_{22} \end{bmatrix}. \tag{15}$$

Eq. (8) can be rewritten:

$$\begin{aligned} [Y_{11}][V_{11}] + [Y_{12}][V_{12}] &= [J_{11}] \\ [Y_{21}][V_{11}] + [Y_{22}][V_{12}] &= [0]. \end{aligned} \tag{16}$$

When voltages are measured in node 1 and node 2 only, the matrix $[V_{12}]$ contains all unknown voltages that are not measured. Elimination of $[V_{12}]$ from Eq. (16) yields:

$$([Y_{11}]-[Y_{12}]\cdot[Y_{22}]^{-1}\cdot[Y_{21}])\cdot[V_{11}]=[J_{11}] \tag{17}$$

or

$$[Y'][V_{11}]=[J_{11}] \tag{18}$$

where

$$[Y']=[Y_{11}]-[Y_{12}]\cdot[Y_{22}]^{-1}\cdot[Y_{21}]. \tag{19}$$

The elements of $[Y']$ are the equivalent admittances to be calculated:

$$[Y']=\begin{bmatrix} y'_{11} & -y'_{12} \\ -y'_{21} & y'_{22} \end{bmatrix}. \tag{20}$$

According to Eq. (3) the equivalent admittances between node 1 and node 2, respectively, and node 0 are given by:

$$y'_{10}=y'_{11}-y'_{12} \quad \text{and} \quad y'_{20}=y'_{22}-y'_{21}. \tag{21}$$

In a similar way the m-node network can be reduced to a 3-node network for other choices of i and j.

When a current step function is used for j_{ii}, and voltages are measured when v_{ij} is time independent, possible capacitive properties of the admittances y_{pq} can be ignored. The admittances are then equal to the conductances and the equivalent resistances can be calculated by:

$$R'_{ij}=1/y'_{ij}. \tag{22}$$

Application to Multicellular Biological Systems

For a multicellular biological system the following assumptions are made:

1. The impedance of a cell membrane can be represented as a resistance in parallel with a capacitance.
2. The cell membrane has no rectifying properties.
3. The resistivity of the cytoplasm and extracellular fluids is negligible.

A system with n compartments (or cells) can be represented as a passive linear network with $m=n+1$ nodes: the surrounding medium (node 0) and n compartments (node 1 to n). Under conditions where the capacitive properties of the membranes can be ignored (*see above*), the interiors of the compartments form the nodes of the network and the junctional and nonjunctional membranes form the conductances y_{pq} or resistances R_{pq} ($R_{pq}=1/y_{pq}$). The conductance y_{pq} or resistance R_{pq} depends on the surface area of the corresponding membrane (A_{pq}) and on the specific resistance of this membrane (r_{pq}):

$$y_{pq}=A_{pq}/r_{pq} \quad \text{or} \quad R_{pq}=r_{pq}/A_{pq}. \tag{23}$$

When the surface areas of the individual membranes (A_{pq}) and the conductances (y_{pq}) are known, Eq. (23) gives the specific resistances. In most biological systems A_{pq} can be estimated from a geometrical model of the system. In principle the y_{pq}'s could be determined from Eq. (7). Since $[Y]$ is symmetrical, there are $1/2\cdot n\cdot(n+1)$ independent y_{pq}'s. Therefore, the number of voltages and currents to be determined experimentally will be too large for most systems to permit the use of Eq. (7) directly. An alternative and much simpler approach is to measure the equivalent resistances R'_{ij}, R'_{i0}, and R'_{j0} in a number of different pairs of cells [4]. When this number is equal to the number of different specific resistances that one assumes to be present, the various specific resistances can be derived by using Eqs. (18) and (23). Starting with arbitrary values for the independent r_{pq}'s and with the estimated values of the surface areas A_{pq}, the resulting equivalent resistances are calculated for each of the pairs of

cells in which these have been measured experimentally. The calculated and experimental values are compared and, if necessary, the initial values of the specific resistances are adjusted by iteration until all experimental and theoretical values agree within certain chosen limits. Fortunately, in most biological systems the number of independent specific resistances will be limited because of symmetry properties or other considerations. As a consequence the number of equivalent resistances to be determined will not exceed the limits of experimental feasibility. In this respect the *Xenopus* embryo is a good example.

The Xenopus Embryo

As in the preceding paper [4], it is assumed that at any time during the development of the *Xenopus* embryo from stage 2 to stage 5 no significant differences exist between the specific resistances of the animal and vegetative parts of a given cleavage membrane. Also, it is assumed that at any time the specific resistance of the membranes enclosing the blastocoel (r_n) is the same and equal to the mean of the specific resistances of the cleavage membranes. From the equivalent junctional and nonjunctional resistances measured it followed that no significant differences exist between the dorsal and ventral parts of a given cleavage membrane, nor between the nonjunctional membranes of different animal cells [4]. Consequently, the independent specific resistances are those of the nonjunctional membrane (r_0) and of the successively formed cleavage membranes (r_i; i=I, II, III, IV, respectively). Thus, the equivalent resistances to be determined are the equivalent nonjunctional resistance between the animal cells and the medium (R'_0) and the equivalent junctional resistances for different adjacent animal cells separated by each of the cleavage membranes (R'_i; i=I, II, III, IV, respectively). A BASIC program was developed for a Wang 2200 B-2 minicomputer, with matrix option, to determine r_0 and r_i from the measured R'_0 and R'_i at the various stages of development, according to the method given above. In the preceding study [4] this program was used to derive r_0 and the various r_i's from the experimentally determined equivalent resistances.

Slight modifications of this program are used to investigate in more detail some of the properties of the *Xenopus* embryo as an electrical network. For details of the geometry of the *Xenopus* embryo and of the notation used to identify individual cells and membranes, *see* Fig. 1 and Ref. [4].

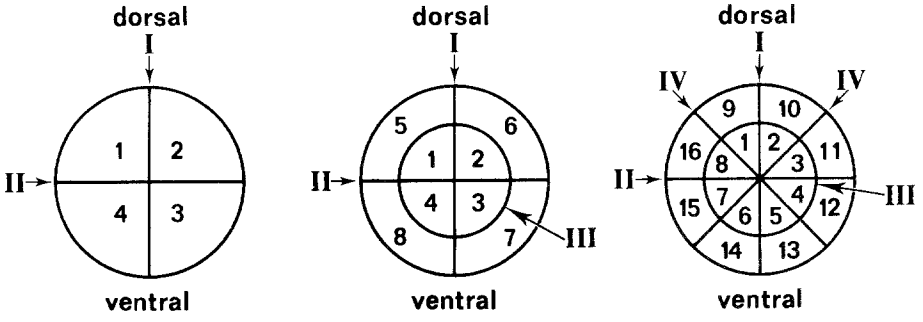

Fig. 1. Diagrammatic representation of the geometry of the 4-, 8-, and 16-cell stages of the *Xenopus* embryo: animal view. The successively formed cleavage membranes are indicated by arrows marked I to IV. The individual cells are numbered separately for each stage

Table 1. Equivalent nonjunctional and junctional resistances (in kΩ) calculated for adjacent cells in the 4-cell, 8-cell and 16-cell embryo[a]

	4-cell embryo	8-cell embryo	16-cell embryo
R'_0	391.2	421.8	478.0
R'_{I}	46.3	88.6	111.9
R'_{II}	46.3	88.6	111.9
R'_{III}	–	76.9	123.4
R'_{IV}	–	–	111.9

[a] The specific resistances of all junctional membranes are equal (r_i, $r_n = 0.4\,\mathrm{k\Omega\,cm^2}$). The specific resistance of the nonjunctional membranes (r_0) has a value of $10\,\mathrm{k\Omega\,cm^2}$. The geometrical parameters are as used in the experimental analysis [4]. R'_0, R'_{I}, R'_{II} and R'_{IV} are given for animal cells only.

Results

In the following sections we will analyze the influence of some of the electrical and geometrical parameters on the properties of the electrical networks formed by *Xenopus* embryos at various stages. For simplicity we use somewhat idealized versions of the embryo. The specific resistances of the junctional membranes are taken to be equal (r_i, $r_n = 0.4\,\mathrm{k\Omega\,cm^2}$), the specific resistance of the nonjunctional membranes (r_0) is put at $10\,\mathrm{k\Omega\,cm^2}$, and the geometrical parameters used for the calculation of the surface areas of the different membranes are as given in the experimental analysis [4], unless indicated otherwise. The equivalent resistances in the 4-, 8- and 16-cell embryo calculated for these conditions are given in Table 1.

The Interpendence of R'_0 and R'_i

The equivalent resistance between two compartments is a measure for the ability to exchange small ions between these compartments, regardless of the pathways chosen by the ionic current. As has been argued [1], and as also can be seen from Eq. (19), in a multicellular system R'_i, and *mutatis mutandis* R'_0, will depend not only on the properties of the junctional membranes but also on those of the nonjunctional membranes. This is understandable since a current flowing from cell to cell via some indirect pathway, in each intermediate cell, has the choice between flowing to an adjacent cell or leaving the system via a nonjunctional membrane. In a two-cell system there is no interdependence of R'_0 and R'_i, since only one pathway exists between each of the three compartments.

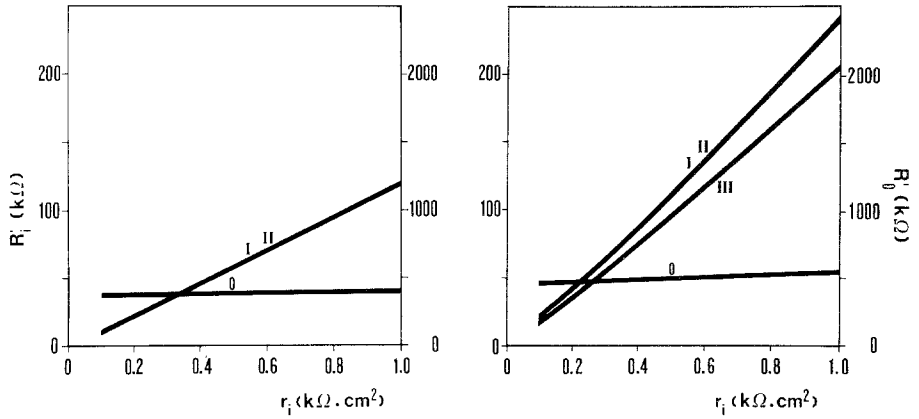

Fig. 2. The equivalent junctional resistances (R_i', i = I, II, III) and the equivalent nonjunctional resistance (R_0') as a function of the specific resistance of the junctional membranes (r_i); r_0 was constant at 10 kΩ cm². In the 8-cell embryo R_I', R_{II}', and R_0' are given for animal cells. Left: 4-cell embryo. Right: 8-cell embryo

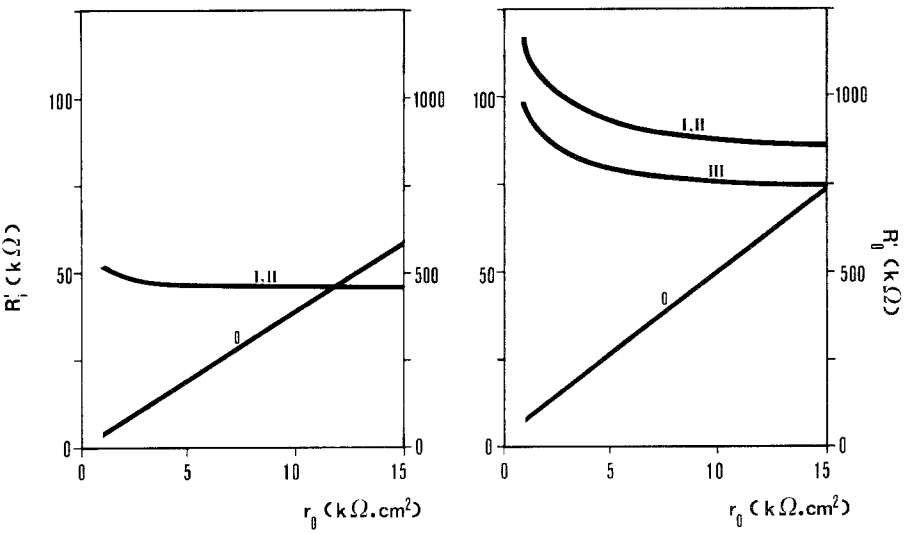

Fig. 3. The equivalent junctional resistances (R_i') and the equivalent nonjunctional resistance (R_0') as a function of the specific resistance of the nonjunctional membranes (r_0); r_i was constant at 0.4 kΩ cm². In the 8-cell embryo R_I', R_{II}', and R_0' are given for animal cells. Left: 4-cell embryo. Right: 8-cell embryo

For the 4- and 8-cell embryo we calculated the influence of r_i and r_0 on the equivalent resistances across the nonjunctional membrane and the various cleavage membranes (Figs. 2 and 3), by varying r_i and r_0 over a range including the span of variation actually measured. It can be seen that R_i' and R_0' show an almost linear dependence on r_i and r_0, respectively, the slope being greater as the number of cells is greater, i.e. as the surface

areas of the individual membranes (A_{pq}) are smaller. From the geometry of the 8-cell embryo it follows that $R'_I = R'_{II}$ and $R'_{III} < R'_I$, R'_{II}. The latter is due to the fact that the surface area of the junctional membrane between adjacent animal and vegetative cells is greater than that of the membrane between two animal cells. The increase in R'_0 with r_i is negligible (Fig. 2), as will be the case in any system where current flows much easier from cell to cell than from cell to medium. The influence of r_0 on R'_i is of more importance in the *Xenopus* embryo (Fig. 3). As r_0 becomes smaller R'_i increases exponentially. Under these conditions coupling is low and the greater part of the excitation current will leak to the medium before it can pass to an adjacent cell. This will result in a large equivalent junctional resistance. The dependence of R'_0 on r_i and of R'_i on r_0 will be greater as coupling decreases. In the *Xenopus* embryo this will occur when the number of cells increases (compare the 4- and 8-cell stage).

The Role of the Blastocoel

The formation of the blastocoel probably starts during the first cleavage cycle. This intercellular cavity is enclosed by the blastomeres and increases in diameter during early development. Morphological observations [3], as well as measurements of the ionic composition of the blastocoelic fluid [10], indicate that a direct pathway between the blastocoel and the medium is absent. During the period of development investigated all cells are in contact with the blastocoel. This cavity could provide an important pathway in intercellular communication. Unfortunately it is hardly accessible to microelectrodes at these stages. In the experimental analysis we therefore made the following assumptions [4]:

1. The specific resistance of the membranes enclosing the blastocoel (r_n) is equal to the mean of the specific resistances of the cleavage membranes (about 0.4 kΩ cm^2).

2. At the 2-cell stage the blastocoel is a sphere with a radius of 0.005 mm. At each cleavage cycle its radius increases by 0.020 mm.

3. The distance (b) between the third cleavage plane and the center of the blastocoel is given by $b = a \cdot x/y$, where x is the radius of the embryo (0.65 mm), y is the radius of the blastocoel, and a is the distance between the third cleavage plane and the center of the embryo (0.01 mm).

The significance of assumptions 1 and 2 was investigated by calculating the equivalent and specific resistances as a function of r_n and y. The equivalent resistances were calculated keeping r_i and r_0 constant at 0.4 kΩcm^2

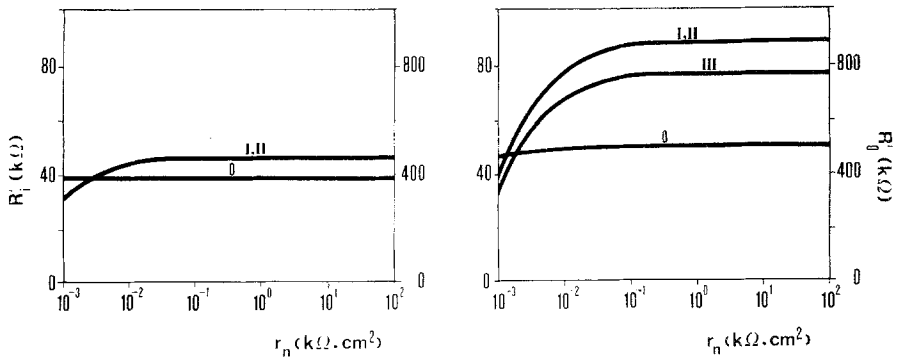

Fig. 4. The equivalent junctional resistances (R_i') and the equivalent nonjunctional resistance (R_0') as a function of the specific resistance of the membranes enclosing the blastocoel (r_n). In the 8-cell embryo R_I', R_{II}', and R_0' are given for animal cells. $r_i = 0.4\ \text{k}\Omega\ \text{cm}^2$, $r_0 = 10\ \text{k}\Omega\ \text{cm}^2$. Left: 4-cell embryo. Right: 8-cell embryo

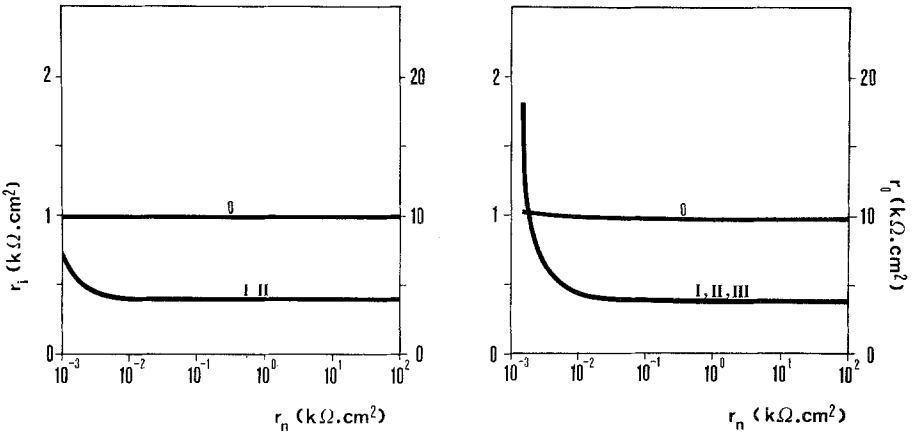

Fig. 5. The specific resistance of the cleavage membranes (r_i) and the specific resistance of the nonjunctional membranes (r_0) as a function of the specific resistance of the membranes enclosing the blastocoel (r_n). The equivalent resistances used are given in Table 1. Left: 4-cell embryo. Right: 8-cell embryo

and $10\ \text{k}\Omega\ \text{cm}^2$, respectively. The specific resistances were derived for the values of R_i' and R_0' given in Table 1.

Figs. 4 and 5 show the influence of r_n on the respective equivalent and specific resistances. It can be seen that under the geometrical conditions chosen the blastocoel is a negligible pathway for values of r_n greater than $0.1\ \text{k}\Omega\ \text{cm}^2$. In the experimental analysis r_n had values of about $0.4\ \text{k}\Omega\ \text{cm}^2$. Therefore, the properties of the blastocoel cannot have influenced the derivation of the specific junctional and nonjunctional resistances. When r_n becomes smaller than $10\ \Omega\ \text{cm}^2$ the equivalent resistances across the

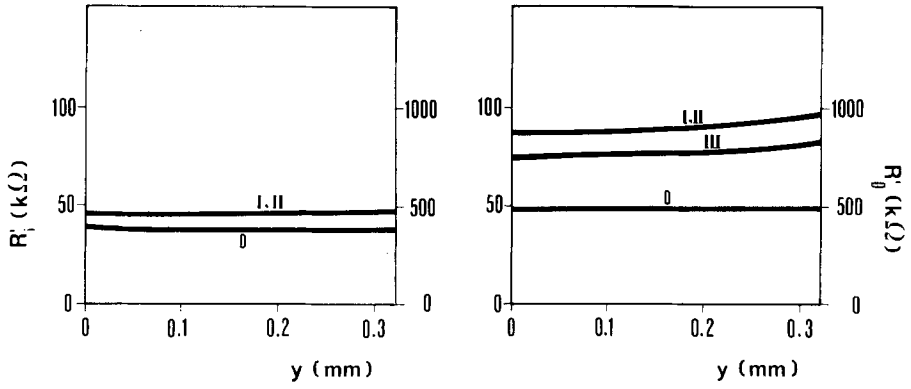

Fig. 6. The equivalent junctional resistances (R_i') and the equivalent nonjunctional resistance (R_0') as a function of the diameter of the blastocoel (y). In the 8-cell embryo R_I', R_{II}', and R_0' are given for animal cells. $r_i = 0.4\ k\Omega\ cm^2$. $r_0 = 10\ k\Omega\ cm^2$. Left: 4-cell embryo. Right: 8-cell embryo

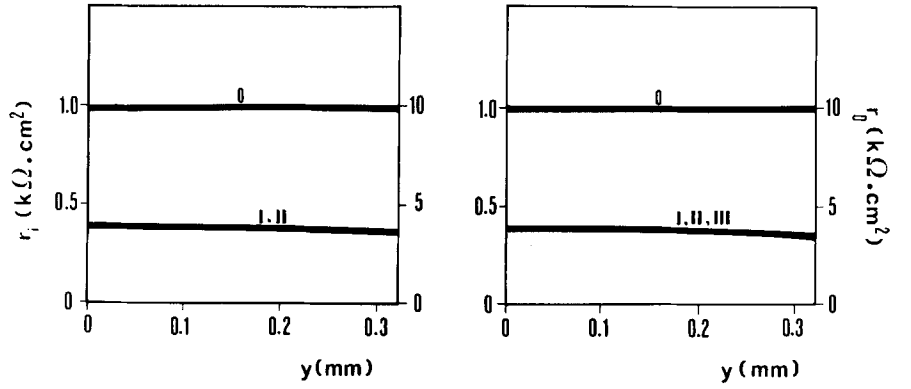

Fig. 7. The specific resistances of the cleavage membranes (r_i) and the specific resistance of the nonjunctional membranes (r_0) as a function of the diameter of the blastocoel (y). The equivalent resistances used are given in Table 1. Left: 4-cell embryo. Right: 8-cell embryo

cleavage membranes decrease strongly, so that the specific resistances of the cleavage membranes would have to increase exponentially in order to explain the equivalent resistances measured. Under these circumstances the blastocoel would form the most important pathway between cells. However, such low values of r_n are not very likely. Special membrane structures would have to be present, and nothing of this kind has been reported [3].

Figs. 6 and 7 show the various electrical parameters as a function of the radius of the blastocoel. An increase in y will have two opposite effects. It will increase the surface areas of the junctional membranes separating

the blastocoel from the cells, thus enhancing coupling between the cells via the blastocoel. On the other hand, the surface areas of the junctional membranes separating the individual cells will decrease, resulting in a decreased coupling between the cells. As can be seen, the overall effect of y is negligible, even when y is equal to 50 % of the radius of the embryo.

Summarizing, we conclude that the choice of the geometrical parameters relative to the blastocoel and the choice of the value of r_n had no influence on the values of r_i and r_0 derived in the experimental analysis. Furthermore, we conclude that the blastocoel does not play a significant role in intercellular coupling at the stages investigated. However, comparing the results obtained for the 4- and 8-cell stage it may be expected that at later stages the blastocoel will form a more important shunt conductance between the cells.

Intercellular Communication in the Early Xenopus Embryo

In the experimental analysis [4] we have measured the equivalent resistances between adjacent compartments only. This was sufficient for the derivation of the specific resistances of the cleavage membranes and the nonjunctional membranes. In the geometrical model it was assumed that the excitation current can only flow directly to adjacent cells, to the blastocoel, and to the medium. No direct current flow was assumed to be possible between diagonally opposed cells, nor between the blastocoel and the medium. On the basis of these assumptions a series of experiments are simulated, using idealized versions of the developmental stages which had been analyzed experimentally [4]. When k is the number of cells per embryo, the values of the following parameters are calculated:

1. The equivalent junctional resistances (R'_{ij}) from one cell (cell i) to all other cells (cell j; $j=1$ to k, $j \neq i$). For the 4-cell embryo: $i=1$. For the 8-cell embryo: $i=1$ (an animal cell); or $i=5$ (a vegetative cell). For the 16-cell embryo: $i=1$ (an animal cell); or $i=9$ (a vegetative cell).

2. The equivalent nonjunctional resistance (R'_{j0}) from cell j to the medium ($j=1$ to k, $j \neq i$).

3. The resulting coupling ratios: $V_j/V_i = 1/(1+R'_{ij}/R'_{j0})$.

The positions of the individual cells are indicated by the numbers 1 to k (Fig. 1). The values for the surface areas of the junctional and nonjunctional membranes were as in the experimental analysis [4]. The specific resistances were chosen as above ($r_0 = 10\ \mathrm{k\Omega\,cm^2}$; $r_i, r_n = 0.4\ \mathrm{k\Omega\,cm^2}$).

The results of these calculations are represented in Figs. 8–12. Some important features of the electrical networks formed by the embryo at

the different stages can be deduced by comparing these Figures. In analyzing them, the geometry of the embryos should be kept in mind (Fig. 1).

The 4-cell embryo consists of four identical cells. Each of these cells is a quadrant of the spherical embryo. Cell 1 is adjacent to cells 2 and 4 and not in direct contact with cell 3 ($A_{13}=A_{24}=0$). In such a symmetrical system the input resistance will be the same for all cells. The input resistance of cell j (v_{j0}/j_{jj}) is formed by R'_{j0} in parallel with ($R'_{ij}+R'_{i0}$). Therefore:

$$v_{j0}/j_{jj}=[(R'_{i0}+R'_{ij})*R'_{j0}]/(R'_{i0}+R'_{ij}+R'_{j0}). \tag{24}$$

As regards the equivalent junctional resistance two classes of cells can be distinguished, i.e. adjacent and nonadjacent cells. Thus, for a given cell i, R'_{ij} depends on j. Since the input resistances of all cells are equal, it follows from Eq. (24) that the equivalent nonjunctional resistances depend on the choice of cell j for a given cell i. However, in all cases $R'_{i0}=R'_{j0}$, because the system is symmetrical.

Fig. 8 shows the results of the calculations for the 4-cell embryo. The difference in equivalent junctional resistances between adjacent cells on the one hand and between nonadjacent cells on the other are small

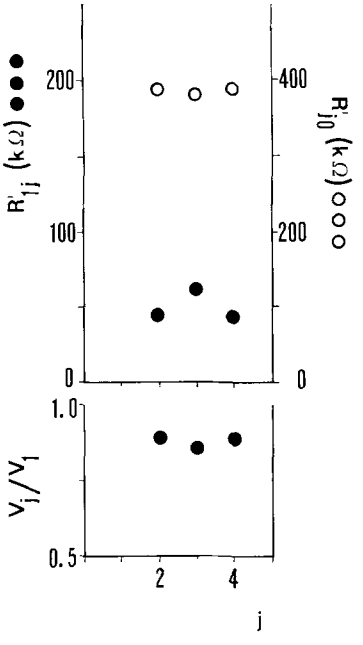

Fig. 8. Simulation of the properties of the electrical network formed by the 4-cell embryo. The equivalent junctional resistances R'_{ij}, equivalent nonjunctional resistances R'_{j0}, and coupling ratios V_j/V_i as a function of j are given for $i=1$. Also, *see text*

($R'_{12}=R'_{14}=46.3\ \mathrm{k\Omega}$; $R'_{13}=62.6\ \mathrm{k\Omega}$), despite the fact that a current has to pass two junctional membranes when flowing from cell 1 to cell 3. Due to this small difference the equivalent nonjunctional resistances for adjacent and nonadjacent cells are almost equal. For adjacent cells, such as cells 1 and 2 or cells 1 and 4, $R'_{i0}=R'_{j0}=391\ \mathrm{k\Omega}$. For nonadjacent cells, such as cells 1 and 3. $R'_{i0}=R'_{j0}=381\ \mathrm{k\Omega}$. The input resistance of all cells is 206 kΩ, as given by Eq. (24). The resulting differences in the coupling ratio V_j/V_i are probably too small to detect experimentally ($V_2/V_1=V_4/V_1=0.89$; $V_3/V_1=0.86$).

The 8- and 16-cell embryos are divided into an animal and a vegetative part, each consisting of four and eight identical cells, respectively. The animal cells are smaller than the vegetative cells. In the 8-cell embryo each of the three cleavage membranes is divided into four equal parts. In the 16-cell embryo the third cleavage membrane is divided into eight equal parts but the other cleavage membranes remain divided into four parts. From this geometry it can be seen that the input resistances will be different for animal and vegetative cells but identical for all cells within each of the two parts. The equivalent junctional resistances fall into three classes dependent on the positions of the cells i and j, i.e., animal-animal cells, vegetative-vegetative cells, and animal-vegetative cells. They will be the same for all adjacent cell pairs within each of these classes, but for nonadjacent pairs R'_{ij} will depend on the choice of j for a given cell i. The differences in R'_{ij} and in input resistance between animal and vegetative cells will lead to differences in the equivalent nonjunctional resistances of different cells j for a given cell i. If the cells i and j are both animal cells or both vegetative cells, $R'_{i0}=R'_{j0}$. However, R'_{i0} will be greater than R'_{j0} if cell i is an animal cell and cell j is a vegetative cell.

Figs. 9 and 10 show the results of the calculations for the 8-cell embryo, for $i=1$ (animal cell) and $i=5$ (vegetative cell), respectively. The outcome of the calculations for the 16-cell embryo is given in Figs. 11 and 12, for $i=1$ (animal cell) and $i=9$ (vegetative cell), respectively. At both stages the minimum value R'_{ij} is found for adjacent vegetative cells (8-cell: $R'_{56}=R'_{58}=65.2\ \mathrm{k\Omega}$; 16-cell: $R'_{9\,10}=R'_{9\,16}=80.1\ \mathrm{k\Omega}$). In the 8-cell embryo R'_{ij} for adjacent animal cells ($R'_{12}=R'_{14}=88.6\ \mathrm{k\Omega}$) is higher than that for adjacent animal–vegetative cells ($R'_{15}=76.9\ \mathrm{k\Omega}$). In the 16-cell embryo the reverse is true ($R'_{12}=R'_{18}=111.9\ \mathrm{k\Omega}$; $R'_{19}=123.4\ \mathrm{k\Omega}$) since the surface areas of the junctional membranes between the animal and vegetative cells are the smaller ones. The largest value of R'_{ij} is found for opposite animal cells (8-cell: $R'_{13}=115.7\ \mathrm{k\Omega}$; 16-cell: $R'_{15}=239.6\ \mathrm{k\Omega}$). In the 8-cell embryo the input resistances for the animal and vegetative cells are 231 kΩ

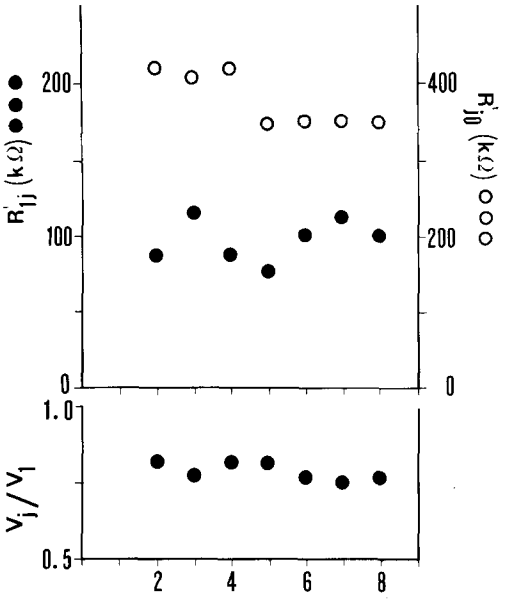

Fig. 9

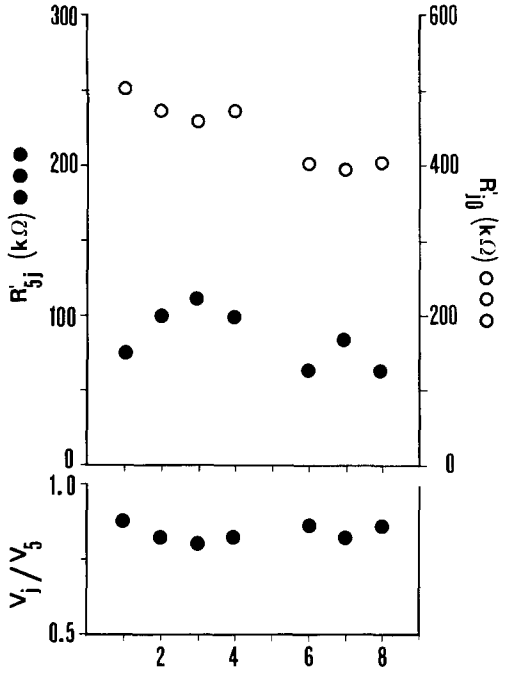

Fig. 10

Figs. 9 and 10. Simulation of the properties of the electrical network formed by the 8-cell embryo. The equivalent junctional resistances R'_{ij}, equivalent nonjunctional resistances R'_{j0}, and coupling ratios V_j/V_i as a function of j are given for $i=1$ (Fig. 9) and $i=5$ (Fig. 10). Also, *see text*

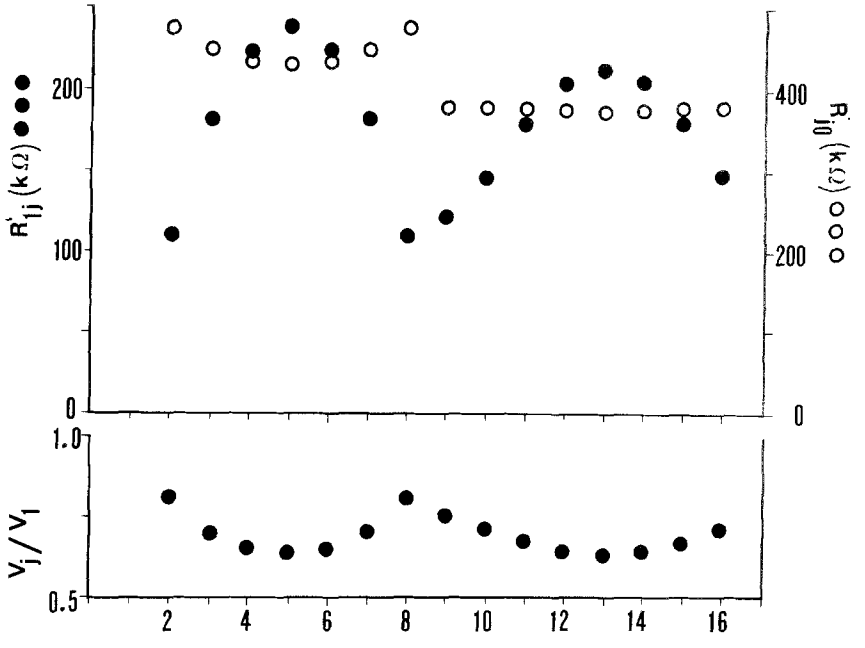

Fig. 11

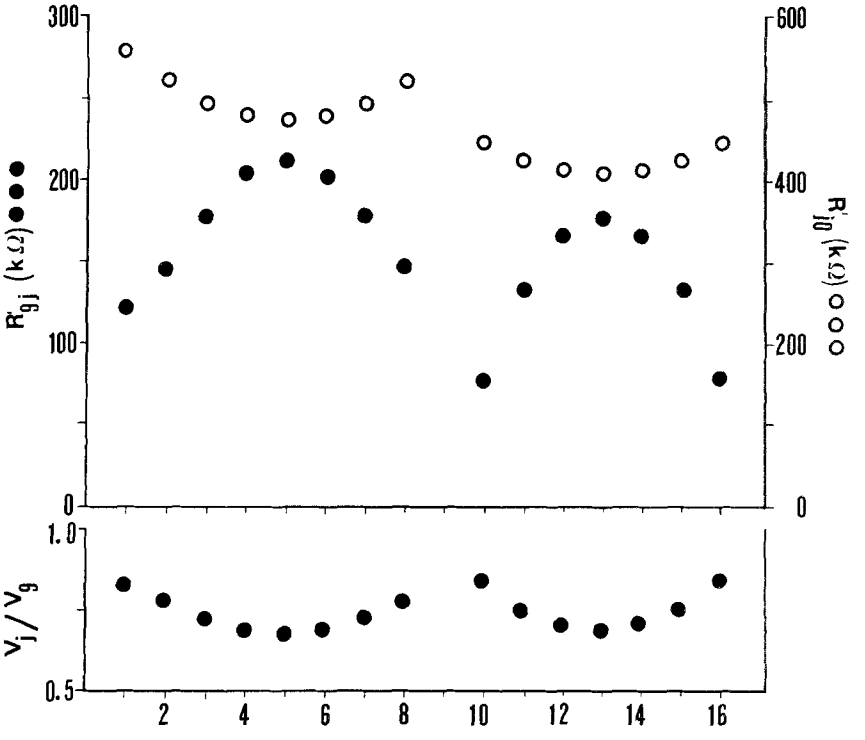

Fig. 12

Figs. 11 and 12. Simulation of the properties of the electrical network formed by the 16-cell embryo. The equivalent junctional resistances R'_{ij}, equivalent nonjunctional resistances R'_{j0}, and coupling ratios V_j/V_i as a function of j are given for $i=1$ (Fig. 11) and $i=9$ (Fig. 12). Also, *see text*

and 218 kΩ, respectively, and in the 16-cell embryo 264 kΩ and 244 kΩ, respectively. The largest difference in equivalent nonjunctional resistance is found in the values calculated for adjacent animal and vegetative cells. In the 8-cell embryo $R'_{j0}=351.0$ kΩ for $i=1$ and $j=5$, and $R'_{j0}=501.8$ kΩ for $i=5$ and $j=1$. In the 16-cell embryo $R'_{j0}=382.2$ kΩ for $i=1$ and $j=9$, and $R'_{j0}=552.8$ kΩ for $i=9$ and $j=1$. The large differences in R'_{ij} and R'_{j0} as a function of the choice of cell i and cell j hardly express themselves in the coupling ratio. In the 8-cell embryo, for $i=1$ this ranges between $V_7/V_1=0.76$ (opposite animal and vegetative cells) and $V_2/V_1=V_4/V_1=0.83$ (adjacent animal cells). For $i=5$ the extremes are $V_3/V_5=0.80$ (opposite animal and vegetative cells) and $V_1/V_5=0.87$ (adjacent animal and vegetative cells). The coupling ratio ranges in the 16-cell embryo for $i=1$ between $V_5/V_1=V_{13}/V_1=0.64$ (opposite animal cells and opposite animal and vegetative cells, respectively) and $V_2/V_1=V_8/V_1=0.81$ (adjacent animal cells). For $i=9$ the minimum value is $V_5/V_9=0.69$ (opposite animal and vegetative cells), while the maximum value is $V_{10}/V_9=V_{16}/V_9=0.85$ (adjacent vegetative cells).

Discussion

In conjunction with a previous experimental study [4] we have analyzed in more detail the properties of the electrical networks formed by the *Xenopus* embryo at the early cleavage stages. The specific resistance of the nonjunctional membranes appeared to be the same for all cells at a particular stage. The specific resistances of the cleavage membranes are most probably equal and remain constant at 400 Ω cm^2. This value is similar to that found for the first cleavage membrane, under conditions at which no membrane junctions are present [5]. Therefore, the electrical data could be explained without assuming the presence of specialized low-resistance junctions, but they could be accounted for equally well by the possible existence of membrane junctions of 0.1 Ω cm^2, e.g. gap junctions, occupying about 0.01 % of the intercellular membranes [4]. Both feasible mechanisms of electrical coupling will give identical results here, provided that the possible junctions are distributed homogeneously over the intercellular membranes.

For simplicity, the theoretical analysis has been given for somewhat idealized versions of the embryos, in which the specific resistances of the cleavage and nonjunctional membranes were put at 0.4 and 10 kΩ cm^2, respectively. However, all calculations were repeated using the actually

measured equivalent resistances and the specific resistances derived from them. This did not influence the conclusions drawn here, but the results were slightly more complicated to interpret.

As emphasized earlier [6], in contrast to two-dimensional systems [7, 8, 9] the geometry of multicellular embryos is not favorable for the derivation of simple equations describing the spreading of current introduced into one cell. The method given here provides an answer to this problem. It is based on the experimental determination of the equivalent resistances between a number of different nodes of the electrical network. Subsequently, the specific resistances can be derived by an iteration procedure, provided the surface areas of the membranes can be estimated. The number of equivalent resistances to be measured depends on the number of independent specific resistances. In most biological systems this will be restricted, and therefore acceptable for an experimental analysis.

The coupling ratio has been commonly used as a measure for intercellular communication. Our results show that the relation between this parameter and the primary membrane properties is a complex one. In a multicellular system the equivalent junctional resistance depends not only on the properties of the junctional membranes but also on those of the nonjunctional membranes. The same holds, *mutatis mutandis*, for the equivalent nonjunctional resistances. This mutual interdependence becomes more important as the coupling ratio becomes smaller (Figs. 2 and 3). Moreover, the equivalent nonjunctional resistance from cell j to the medium (R'_{j0}) does not merely depend on the choice of j; it depends on the choice of both cell i and cell j, in which currents are applied and voltages are measured for the determination of the equivalent resistances (compare Figs. 9 and 10, 11 and 12).

In the early *Xenopus* embryo the blastocoel is the only compartment in which direct measurements with microelectrodes are impossible without causing substantial damage to the embryo. Also, detailed information on the geometry of the blastocoel is lacking. We therefore had to make certain assumptions regarding the blastocoel and the membranes enclosing it. The possible influence of these assumptions was tested in simulation experiments (Figs. 4–7). We conclude that it is unlikely that the blastocoel plays a significant role in intercellular communication at the stages investigated. However, comparing the results obtained for the 4-cell and 8-cell embryo, it may be expected that at later stages the blastocoel will form a more important shunt conductance between the cells.

In the experimental analysis we had measured the equivalent resistances in adjacent cells only, because we assumed that the excitation current

cannot flow directly to nonadjacent compartments [4]. Based on this assumption the equivalent resistances between all possible pairs of cells and the corresponding coupling ratios were calculated. The results were given for all pairs that can be formed with one cell of the 4-cell embryo and for all pairs that can be formed with an animal or vegetative cell, respectively, in both the 8-cell and the 16-cell embryo (Figs. 8–12). From the symmetry of the embryo it follows that all other combinations can be derived from these figures. The large difference between the specific resistance of the junctional and nonjunctional membranes in combination with the existence of several parallel pathways between any two cells, keeps the differences in equivalent resistance and coupling ratio between adjacent and non-adjacent cells relatively small. These differences become more pronounced as development proceeds, since the decrease in surface area of the junctional membranes and the increase in their number result in a drastic increase of the junctional resistances. For the same reason the equivalent resistance between comparable cell pairs, such as adjacent cells or diagonally opposed cells, increases during development.

If the specific resistances of all junctional membranes are equal, R'_{III} will be smaller than R'_{I} and R'_{II} at the 8-cell stage, and greater than R'_{I}, R'_{II}, and R'_{IV} at the 16-cell stage. The calculated differences are small (Table 1). In the experiments no statistically significant differences could be detected [4]. These small differences were either obscured by the large variation in the equivalent resistances at any one stage, or they were introduced by our geometrical modelling.

Two earlier studies have been made of electrotonic coupling in *Xenopus* embryos of comparable stages. Palmer and Slack [6] measured input resistances and voltage decay at various stages. No data on the specific membrane resistances were derived. The input resistance decreased during the first two or three division cycles, then remained relatively constant, and increased drastically during later blastula stages. As development proceeded the coupling ratio between adjacent cells decreased, and voltage decayed more quickly as a function of the number of cell junctions intervening between two cells. These findings are in accordance with our results. Recently, DiCaprio, French and Sanders [2] analyzed the electrical networks formed by the 2-cell and the 4-cell stage. These authors measured frequency response functions between cells, a technique particularly useful for the investigation of the capacitive properties of cell membranes. However, in *Xenopus* embryos the junctional membranes constitute negligible capacitances, so that in this case the advantages of the method are limited. Some important discrepancies exist between their results

and ours [4]. The mean value of the junctional resistance at the 2-cell stage was found to be 286 kΩ, which is about an order of magnitude larger than that found by us. In conjunction with this high junctional resistance, the mean value for the coupling ratio was reported to be 0.772 at this stage. Neither Palmer and Slack [6] nor we [4] found such low values for the coupling ratio prior to the 8-cell stage. However, based on the example DiCaprio *et al.* gave for a measurement in the 2-cell embryo we calculated a coupling ratio of 0.92. The origin of these discrepancies is not clear. DiCaprio *et al.* emphasized that in the 4-cell stage two classes of cell pairs can be distinguished: adjacent pairs and diagonal pairs. Frequency response curves were measured in both classes. Mainly on the basis of the equality of the high-frequency gain asymptote for both classes, they concluded that all cells are interconnected by equal resistances, including the diagonal pairs. They assume that special junctions are involved in the coupling between diagonal pairs. Morphological evidence for the existence of a contact area between diagonally opposed cells is given. The authors show a scanning electron-micrograph of the animal pole and a light micrograph of a section through the vegetative hemisphere, to illustrate that the diagonal pairs are morphologically connected: one pair at the animal pole and the other at the vegetative pole. For several reasons we are not convinced by the evidence presented. A statistical comparison of the data obtained for adjacent and diagonal pairs is lacking. Also in the 4-cell embryo the reported junctional resistance is much higher than that found by us [4]. Moreover, based on our observations of the morphology of a large number of *Xenopus* embryos at the 4-cell stage, the illustrations given by DiCaprio *et al.* [2] appear to show a coincidence rather than a common feature of *Xenopus* embryos. Some embryos do indeed show the diagonal connections described, others do so only between one diagonal pair of cells, while embryos can also be found which lack any diagonal connection. Taking all this into account, the much simpler model in which direct current flow is possible between adjacent compartments only is to be preferred.

We thank Mrs. M. M. Marques da Silva Pimenta Guarda and Mr. M. A. da Silva Guarda for their technical assistance, Miss E. Bartova for preparing the drawings and Mr. L. Boom and Mrs. E. G. Aleven for the photography. We are grateful to Dr. J. Faber and Professor P. D. Nieuwkoop for a critical reading of the manuscript.

References

1. Bennett, M. V. L. 1966. Physiology of electrotonic junctions. *Ann. N. Y. Acad. Sci.* **137**:509
2. DiCaprio, R. A., French, A. S., Sanders, E. J. 1974. Dynamic properties of electrotonic coupling between cells of early *Xenopus* embryos. *Biophys. J.* **14**:387

3. Kalt, M.R. 1971. The relation between cleavage and blastocoel formation in *Xenopus laevis* II. Electron microscopic observations. *J. Embryol. Exp. Morph.* **26**:51
4. de Laat, S.W., Barts, P.W.J.A., Bakker, M.I. 1976. New membrane formation and intercellular communication in the early *Xenopus* embryo. I. Electrophysiological analysis. *J. Membrane Biol.* **27**:109
5. de Laat, S.W., Bluemink, J.G. 1974. New membrane formation during cytokinesis in normal and cytochalasin B-treated eggs of *Xenopus laevis*. II. Electrophysiological observations. *J. Cell Biol.* **60**:529
6. Palmer, J.F., Slack, C. 1970. Some bio-electric parameters of early *Xenopus* embryos. *J. Gen. Physiol.* **24**:535
7. Shiba, H. 1971. Heavyside's 'Bessel cable' as an electric model for flat simple epithelial cells with low resistive junctional membranes. *J. Theor. Biol.* **30**:59
8. Shiba, H., Kanno, Y. 1971. Further study of the two-dimensional cable theory: An electric model for a flat thin association of cells with a directional intercellular communication. *Biophysik* **7**:295
9. Siegenbeek van Heukelom, J., Denier van der Gon, J.J., Prop, F.J.A. 1972. Model approaches for evaluation of cell coupling in monolayers. *J. Membrane Biol.* **7**:88
10. Slack, C., Warner, A.E., Warren, R.L. 1973. The distribution of sodium and potassium in amphibian embryos during early development. *J. Physiol.* **232**:297